Title
DEVELOPMENT OF THE HE-JET FED ON-LINE MASS SEPARATOR RAMA, II

Author
Moltz, D.M.

Publication Date
1979-12-01

UC-37 + [illegible]
LBL-9721 c.1
Preprint

Lawrence Berkeley Laboratory
UNIVERSITY OF CALIFORNIA

Submitted to Nuclear Instruments and Methods

DEVELOPMENT OF THE HE-JET FED ON-LINE MASS SEPARATOR RAMA, II

D. M. Moltz, J. M. Wouters, J. Äystö, M. D. Cable,
R. F. Parry, R. D. von Dincklage, and J. Cerny

December 1979

NUCLEAR SCIENCE DIVISION

Prepared for the U.S. Department of Energy under Contract W-7405-ENG-48

DISCLAIMER

LBL-9721

DEVELOPMENT OF THE HE-JET FED ON-LINE MASS SEPARATOR RAMA, II*

D. M. Moltz, J. M. Wouters, J. Äystö,† M. D. Cable,
R. F. Parry, R. D. von Dincklage,‡ and Joseph Cerny

Department of Chemistry and
Lawrence Berkeley Laboratory
University of California
Berkeley, California 94720

December 1979

Abstract:

Improvements to the on-line mass separator RAMA have permitted a substantial increase in total yield. This increase was achieved by an ion source redesign that improved the total efficiency of the system as well as by an increase in activity from utilizing a multiple-capillary multiple-target system. Successful observation of the exotic light nuclei ^{20}Mg and ^{24}Si indicates an observable cross-section of approximately 1 μb for activities in the 100 ms half-life regime.

---

*This work was supported by the Nuclear Physics and Nuclear Sciences Divisions of the U. S. Department of Energy under contract No. W-7405-ENG-48.

†On leave from: University of Jyväskylä, Finland.

‡Present address: University of Göttingen, W.-Germany.

1. Introduction

The versatility of the on-line mass separator RAMA has already been demonstrated[1,2]. The basic system, however, had some features which made its operation ineffective. It was evident that the operating conditions of the helium-jet system had not been totally optimized. Further, the ion source was excessively long, making the acceptance of the skimmed activity cone necessarily small; finally, the accelerating and extracting potential could not be maintained above 11 kV without breakdown of primary insulators. Since the overall efficiency of the RAMA system described in the preceding paper[1] was neither optimal nor always consistent, it was of interest to improve the operating conditions.

One of the original objectives of the RAMA system was to study the decay of the $A = 4n$, $T_z = -2$ series of beta-delayed proton emitters. In the search for ^{40}Ti via the ^{40}Ca(^{3}He,3n) reaction by Sextro, et al.[3], only protons from the known beta-delayed proton emitters ^{37}Ca and ^{41}Ti, produced in much higher yield in the competing (^{3}He, α2n) and (^{3}He,2n) reactions, were observed. This was a typical result of such searches so that mass separation was clearly needed. The (^{3}He,3n) reactions were expected to have production cross sections such that effective observable cross sections of 1 μb were of interest. Considerable improvement in total yield was thus needed to make these studies possible. Though our discussion will continue to use the search for these beta-delayed proton emitters as an example, the ability to observe low yield, short half-life species is of general interest in the study of nuclei far from stability.

Figure 1 presents a schematic diagram of the RAMA system with these improvements to the helium-jet and the ion source. The first improvement was the addition of a multiple capillary, multiple target approach to recoil atom collection employing a cooled collection cylinder and nitrogen gas-cooled-entrance and exit windows. The second major improvement was a total redesign of the ion source region including shortening the ion source by more than a factor of two. This report will center primarily on discussing these two improvements in addition to a brief account of the new detector systems developed for studies of the quite short-lived ($\sim$100 ms) $T_z = -2$ beta-delayed proton emitters.

2. Multiple Capillary System

In a traditional one-capillary gas-jet system, the total transport yield for short-lived ($t_{1/2}$ < 500 ms) and long-range (> 1 cm) recoil atoms is limited due to the relatively large gas volume needed to stop the recoils. Since many light nuclei far from stability have half-lives in the 100 ms regime, improvements to increase the yield of short-lived activities from the helium-jet system had to be considered. A multiple capillary system was designed for both gas and solid targets to increase the total target thickness for optimum recoil production.

The multiple capillary system employed for gas targets is shown schematically in fig. 2. In this case the transport gas also serves as the target medium. Nuclear reaction recoils are thermalized in the collection cylinder, collected by a set of adjacent capillaries evenly spaced in the side of this cylinder, and then sent to a junction. A single 6 m long stainless steel capillary transports the activity from the junction to the skimmer-ion source region. The total yield exiting from the helium-jet system is given by:

$$\text{YIELD} \equiv Y = \sigma' \cdot N \cdot \Delta V_o e^{-\ell n 2 (t_d / t_{1/2})} \qquad (1)$$

where t_d ≡ the total delay time

$t_{1/2}$ ≡ half-life of the activity of interest

ΔV_o ≡ active collection volume per capillary

N ≡ number of capillary tubes

σ' ≡ the effective cross section thermalized in ΔV_o.

The total delay time is a sum involving the effective sweep-out time of the total collection volume $N \cdot \Delta V_o$, the multiple capillary delay time,

and the delay time in the main capillary tube. It is given by

$$t_d \approx \frac{N \cdot \Delta V_o}{Q} + \frac{\bar{L}_M}{\bar{v}_m} + \frac{2}{3}\frac{L}{v_o}, \qquad (2)$$

where $Q \equiv$ flow rate

$\bar{L}_M \equiv$ average capillary length in the multiple capillary system

$\bar{v}_m \equiv$ average velocity in the multiple capillary system $= 4Q/N\pi D_M^2$

$L \equiv$ length of the main capillary

$v_o \equiv$ initial gas velocity in the main capillary

$D_M \equiv$ diameter of a single capillary in the multiple capillary system.

The last term in equation (2) is an approximation[4]. Additionally, the very small delay time in the junction has been ignored. If we assume $L_M \lesssim 0.01 \cdot L$ and $D_M \lesssim D$ (where D is the diameter of the main capillary tube), the delay time in the multiple capillary system is small and the total delay time can be approximated by

$$t_d \approx \frac{1}{Q}\left[\frac{\pi}{6} L D^2 + N \cdot \Delta V_o\right]. \qquad (3)$$

An illustration of the effective yield of a nuclear reaction as a function of the number of capillaries and the species half-life is given in fig. 3. By substituting either measured quantities or reasonable estimates for all parameters in equation (1), the relationships for two different 6 m long capillary tubes (1.0 and 1.4 mm ID) for two different half-lives are obtained. For very short-lived activities, the improved production is limited by the longer transport times associated with a multiple capillary system. A yield calculation under such conditions for a 1 mm ID capillary shows that the yield for a nuclide with a 122 ms half-life (^{21}Mg) increases by a factor of four when a single capillary is replaced by a ten-capillary system. An overall increase of a factor of 10 results when the same ten-capillary system feeds a 1.4 mm main capillary tube. These calculations were experimentally checked with ^{20}Na and ^{21}Mg produced in the ^{20}Ne(^{3}He,p2n) and ^{20}Ne(^{3}He,2n) reactions at a bombarding energy of 40 MeV. The target employed was spark-chamber gas (90% Ne + 10% He) which for these experiments served both as the stopping and the transport medium. The results were in good agreement with the curves given in fig. 3.

Similar considerations for a solid target system change to some degree with each projectile-target combination because of the differing range-energy behavior of the recoiling compound nuclei. Light ion projectiles normally lose relatively little energy in traversing a target which is one compound nucleus recoil distance thick making the effective bombarding energy the same throughout, while heavy ion projectiles lose much greater amounts of energy in traversing the system (target plus gas) creating a substantial bombarding energy gradient and often a dramatic cross section change. These conditions were empirically optimized by maximizing the number of targets which could be effectively utilized with the choice of an overall 8-12

capillary system. The twelve-capillary, three target system shown in Fig. 4 was thus constructed for light ion reactions such as would be needed for the studies of A=4n, T_z = -2 nuclides. The four capillaries for each target provide collection from approximately one recoil range for compound nuclei formed at the back of a target. This increase in the effective collection volume for each target multiplied by the three targets again provided nearly a tenfold increase in yield. A further, ten-capillary two-target system was constructed to accommodate target-projectile combinations in which the projectile ranged from ^{10}B to ^{20}Ne. For incoming projectiles heavier than ^{20}Ne, a ten capillary system is used with a single target. The overall mean transport times for all of these multiple capillary systems have been measured with the 446 ms beta-delayed alpha-particle emitter ^{20}Na by pulsing the cyclotron on for 0.1 s and off for 3 s. The observed transport times are listed in Table I. The overall He-jet efficiencies were typically above 10% as determined earlier[1].

As was mentioned in the previous paper[1], the opening angle for the heavy mass clusters needs to be $\leq 2^{\circ}$ to reach the plasma region of the ion source. Ethylene glycol has traditionally been used as our additive for efficient transport for the RAMA helium-jet because it most effectively met this small opening angle criterion. The results, however, were not as reproducible as might be desired. The transport efficiency at low beam intensities has been observed to depend on the beam current passing through the helium in a manner scaling approximately as $[dE/dx]^{-1}$ for the different projectiles. A general capability for handling increased beam on target was then necessary to improve the transport efficiency as well as to increase the actual production. Unfortunately, for heavier projectiles, the entrance

and exit windows failed when too high current beam was incident. To permit a nominal beam trebling, double-windowed entrance and exit foils were incorporated into the system (see fig. 1), by which cold nitrogen gas could be directed onto the windows. This process also cooled the He-jet region to temperatures near or below $0^{o}C$. This cooling caused the opening angle to decrease (i.e., the cluster size had apparently increased), improving the transmission of activity through the skimmer into the ion source. However, if the gas temperature and the temperature of the collection cylinder differed greatly, a total extinction of yield was noted. Thus an independent cooling of the cylinder was introduced. The optimum gas temperature region for ^{3}He induced reactions appeared to be $\sim 0 \pm 10\ ^{o}C$, and an optimal cylinder temperature needed to be maintained within ten degrees of this value.

3. Ion Source Region

Two major goals in the redesign of the ion source were to decrease the distance between the capillary exit and the plasma region and to raise the accelerating potential to 18 kV from the 11 kV limit necessitated earlier by the existing high voltage insulators. Given the design criterion that the critical internal dimensions of our hollow-cathode ion source must remain intact, a modified ion source and its holder as shown in fig. 5 were developed. This new ion source is only 9 cm long, as compared with ∿21 cm for the original. Elimination of the focusing solenoid (which was found to be ineffective) helped produce a larger acceptance angle (see previous paper[1]) and provided space for better vacuum pumping in the extraction region, thereby reducing scattering between the ions and spectator neutral molecules (or atoms). The extractor and Einzel lens assemblies of the original RAMA design were left unchanged.

Tests with internally produced 18 keV beams of $^{40}Ar^{+}$ and $^{20}Ne^{+}$ showed that the system could be operated for long periods of time with no apparent changes in beam characteristics. As an example of the resolution obtainable with this improved ion source, a channeltron electron multiplier scan of the stable tin isotopes between masses 114 and 122 is shown in fig. 6. The observed resolution at full-width one-tenth maximum has increased to 304 (from 194, see ref. 1). Since all of the optical parameters were found to scale by either $\sqrt{\frac{E_F}{E_I}}\left(\sqrt{\frac{18}{10.5}} = 1.31\right)$ for magnetic elements or $\frac{E_F}{E_I}$ (1.71) for electrostatic elements, this increase in resolution can be attributed to a lowered ion source emittance, the reduced pressure in the extractor region, and the reduced space charge effects at this beam energy.

Tests with radioactivity were also performed to determine the effects of these changes on the actual throughput of the ion source. The results of increasing the extraction potential from 10.5 to 18 kV were checked with the rare-earth alpha particle emitter ^{153}Er produced in the ^{142}Nd(^{16}O,5n) reaction at 105 MeV; an increase in yield of a factor of about five was observed.

Extensive tests performed with the beta-delayed alpha-particle emitter ^{20}Na produced by the ^{20}Ne(^{3}He,p2n) reaction at 40 MeV showed that the ion source efficiency for sodium had increased a factor of approximately three. The total increase in the ^{20}Na yield on the focal plane was then nearly 30 due to a further factor of ten from the improved He-jet yield. Table II lists examples of RAMA ion source efficiencies for short lived isotopes of Na, Mg, and Si. The higher efficiency obtained for Na can be explained by its high volatility and easy surface ionization.

4. Detection System Improvements

Due to the expected low yields on the RAMA focal plane for many of the reaction products of interest, large solid angle detector systems are a necessity in increasing the overall efficiency. Such a system for charged particle detection (incorporating two detector telescopes for reasons noted below) was developed as shown in fig. 7; this system possesses a detection efficiency of 38% of 4π for higher energy particles. The original telescope used 300 $\mu g/cm^2$ Kimfoil catcher foils (see ref. 1) rather than the carbon foils shown. These thick Kimfoils proved to degrade the energy of the protons (observed in beta-delayed proton decay) and thus broaden the measured peak width. The present system with 2×25 $\mu g/cm^2$ carbon foils was subsequently incorporated.

A method to measure the half-life of very short-lived nuclides (< 200 ms) was also needed, but any mechanical device to move the activity is generally fairly slow. Even the flipper wheels discussed in ref. 1 with the $\sim$ 40 ms flip times could not be operated on a 200 ms timescale without consistent mechanical failure due to the violent nature of stopping such a rotation. However, introducing the capability of fast vertical switching of the beam between the double stack of telescopes shown in fig. 7 permits two collection-counting cycles while losing almost no data. The RAMA beam can be flipped from an "up" to a "down" position by reversing the polarity on the vertical deflection plates shown in fig. 1. This polarity change is accomplished by a fast driven vacuum tube system which has been tested at a 100 μs cycle time even though nominal

flip sequences are on the order of 200 ms. Since the resultant deflection on the focal plane is $\sim \pm$ 2cm from the central plane, this deflection does not seriously affect the optical properties. The technique was proven to work well by remeasuring the 446 ms half-life of ^{20}Na [5].

5. Summary

Redesign of the ion source and addition of a multiple capillary-multiple target arrangement to our basic helium-jet fed on-line mass analysis system has resulted in a substantial increase in the overall yield. These improvements have led to experiments observing for the first time the beta-delayed proton decay of two members of the $T_z = -2$, $A = 4n$ series of light nuclides, ^{20}Mg and ^{24}Si[5,6]. These results show that activities with effective cross sections of 1 μb and half-lives of ∿100 ms can indeed be studied with RAMA. RAMA has also been demonstrated to be a versatile instrument. Elements (ions) so far observed as activity on the RAMA focal plane include Na^+, Mg^+, Si^+, Al^+, P^+, K^+, In^+, Ag^+, Cd^+, Sn^+, Sb^+, Te^+, I^+, Cs^+, Ba^+, Tb^+, Dy^+, Ho^+, Er^+, Tm^+, and At^+.

Footnotes and References

1) D. M. Moltz, R. A. Gough, M. S. Zisman, D. J. Vieira, H. C. Evans, and Joseph Cerny, Nucl. Inst. Meth., previous article, Report No. LBL-9476.

2) Joseph Cerny, D. M. Moltz, H. C. Evans, D. J. Vieira, R. F. Parry, J. M. Wouters, R. A. Gough, and M. S. Zisman, in Proceedings of the Isotope Separator On-Line Workshop, edited by R. E. Chrien, Brookhaven National Laboratory, 1977, BNL-50847, p. 57.

3) R. G. Sextro, R. A. Gough, and Joseph Cerny, Nucl. Phys. A234 (1974) 130.

4) H. Dautet, S. Gujrathi, W. J. Wiesehahn, J. M. D'Auria, and B. D. Pate, Nucl. Instr. Meth. 107 (1973) 49.

5) D. M. Moltz, J. Äystö, M. D. Cable, R. D. von Dincklage, R. F. Parry, J. M. Wouters, and Joseph Cerny, Phys. Rev. Lett. 42 (1979) 43.

6) J. Äystö, D. M. Moltz, M. D. Cable, R. D. von Dincklage, R. F. Parry, J. M. Wouters, and Joseph Cerny, Phys. Lett. 82B (1979) 43.

Figure Captions

Fig. 1. Overall schematic diagram of the present RAMA system.

Fig. 2. Schematic diagram of the gas target multiple capillary system.

Fig. 3. Theoretical yield for two nuclides of interest comprising a short- and a longer-lived activity as a function of the number of capillary tubes in a multiple capillary system. In these calculations spark chamber gas (90% Ne + 10% He) was used as a transport gas. Further details are given in the text.

Fig. 4. Schematic diagram of the solid target multiple capillary system used for light-ion reactions.

Fig. 5. Schematic diagram of the new RAMA ion source region.

Fig. 6. Channeltron electron multiplier scan of stable tin isotopes from mass 114 to 122 at 18 kV.

Fig. 7. Schematic diagram of the RAMA focal plane incorporating solid-state detector telescopes for measuring the decay properties of short-lived heavy particle emitters. Changing the beam from the "up" to the "down" position on a cyclical basis permits half-life determinations.

Table I. Experimental Total Transport Times for Various Capillary and Target Systems

Transport Gas	Target System (Includes multiple capillaries)	Main Capillary Diameter (mm)	Mean Transport Time (ms)
Helium	2 Targets[a)]	1.0	520
Helium	3 Targets[b)]	1.0	540
Helium	2 Targets[a)]	1.4	180
Helium	3 Targets[b)]	1.4	200
Neon	Gas Target[c)]	1.4	300

a) 5 1.0 mm i.d. capillaries per target

b) 4 1.0 mm i.d. capillaries per target

c) 12 1.0 mm i.d. capillaries; spark chamber gas (90% Ne + 10% He) was used

Table II. RAMA Ion Source Efficiencies

^{20}Na	^{21}Mg	^{25}Si
0.6 %	0.1 %	0.1 %

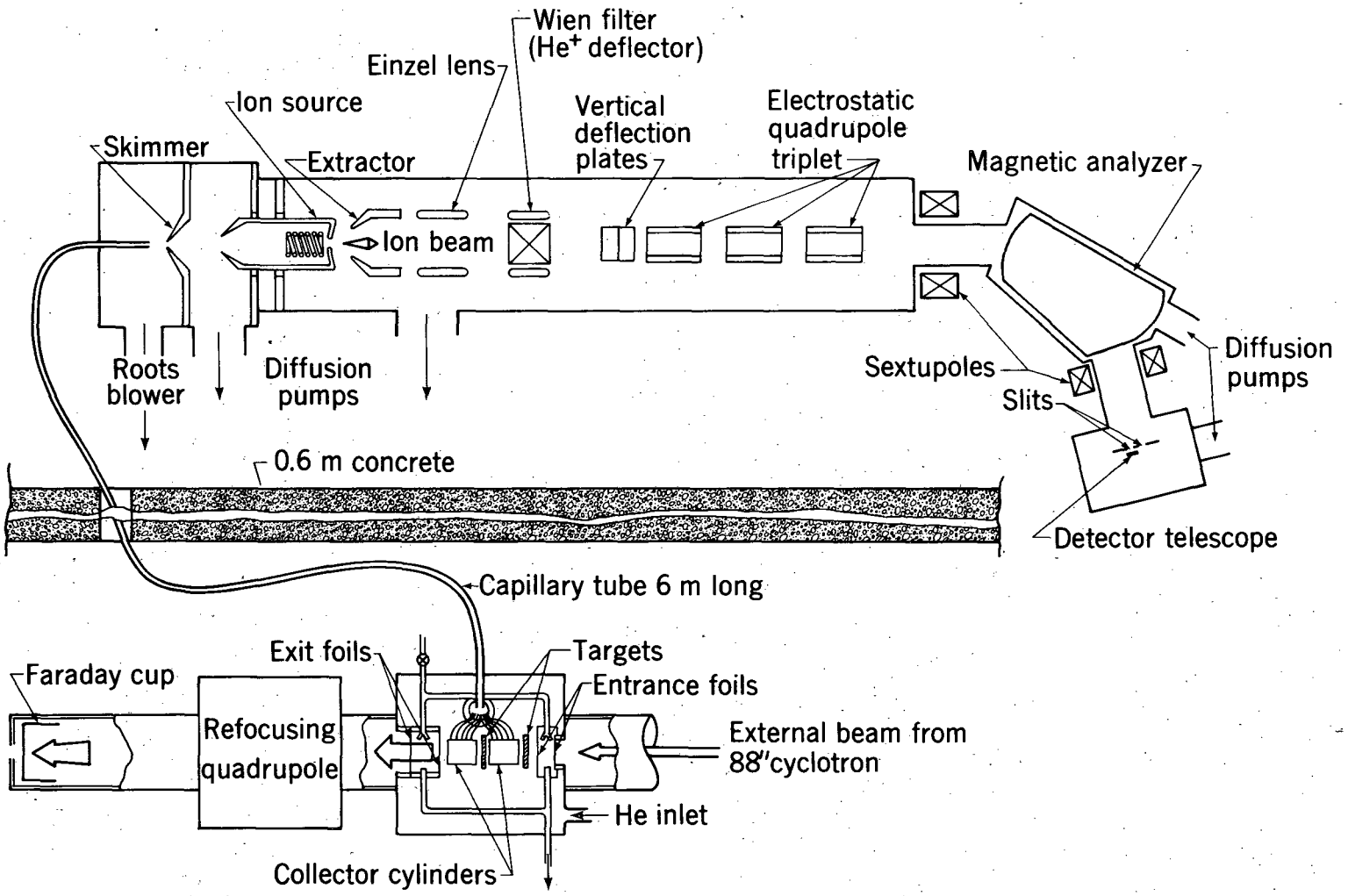

RAMA - 88 SCHEMATIC

Fig. 1

XBL7811-12583

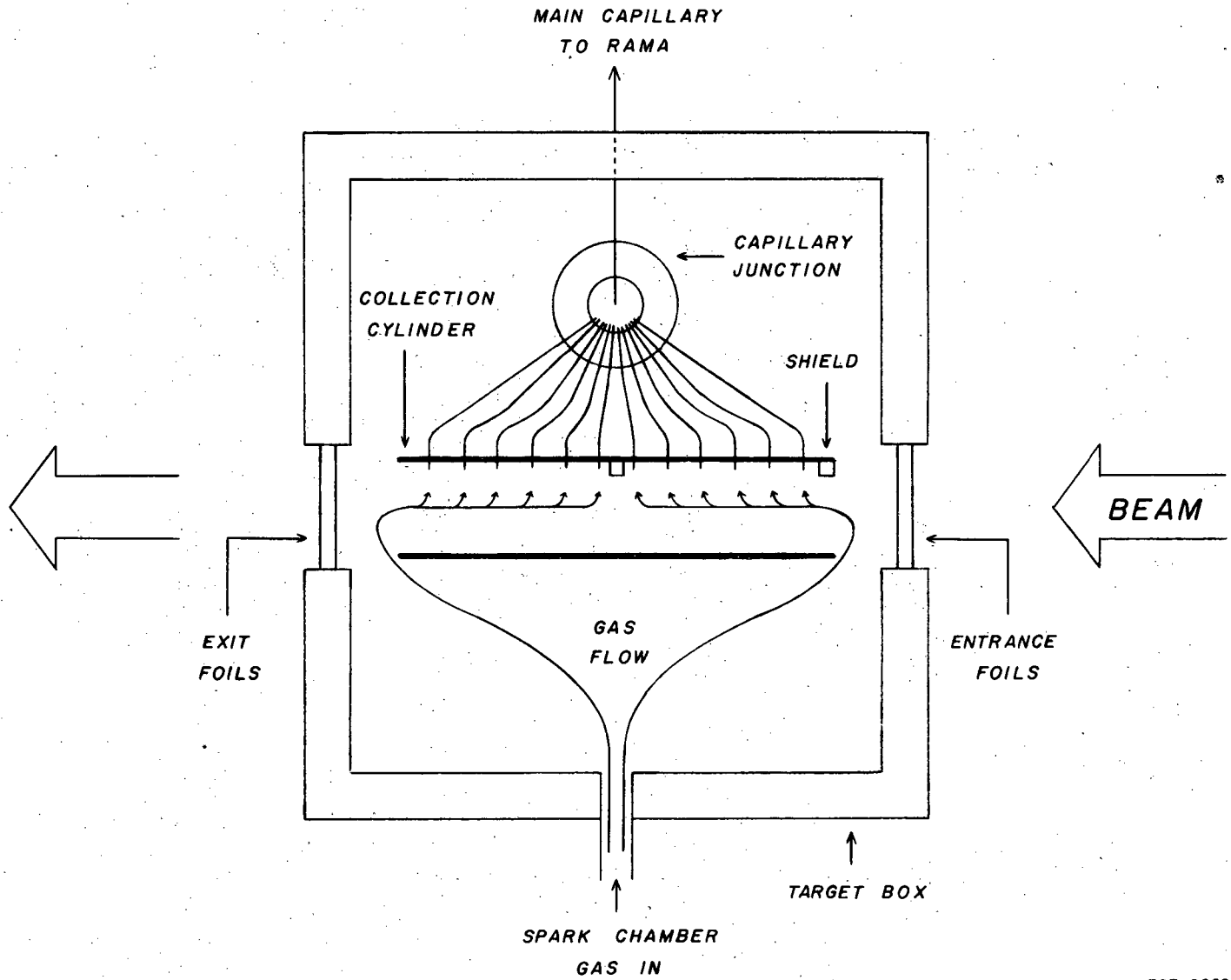

XBL 787-9660

Fig. 2

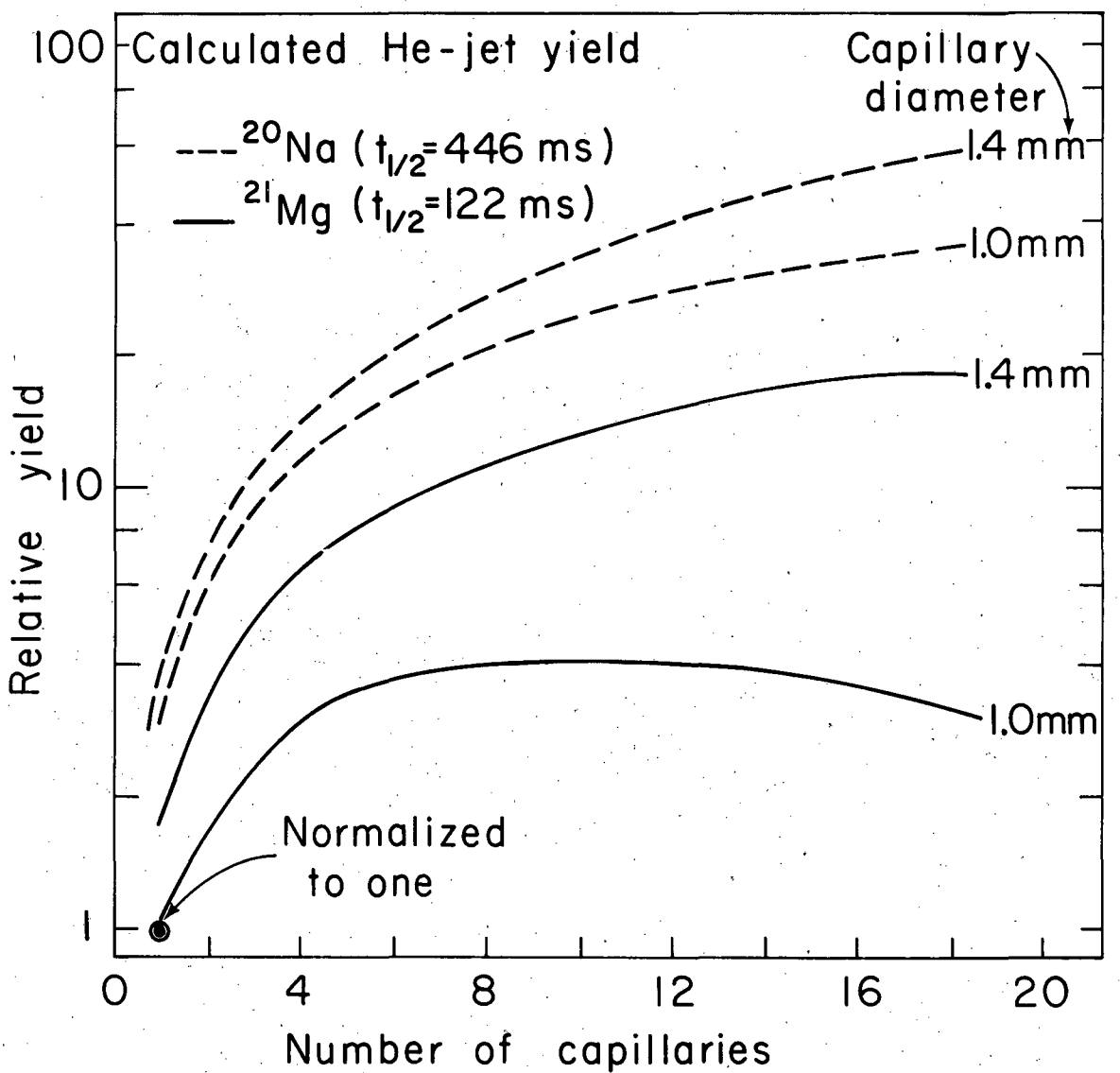

XBL 791-30

Fig. 3

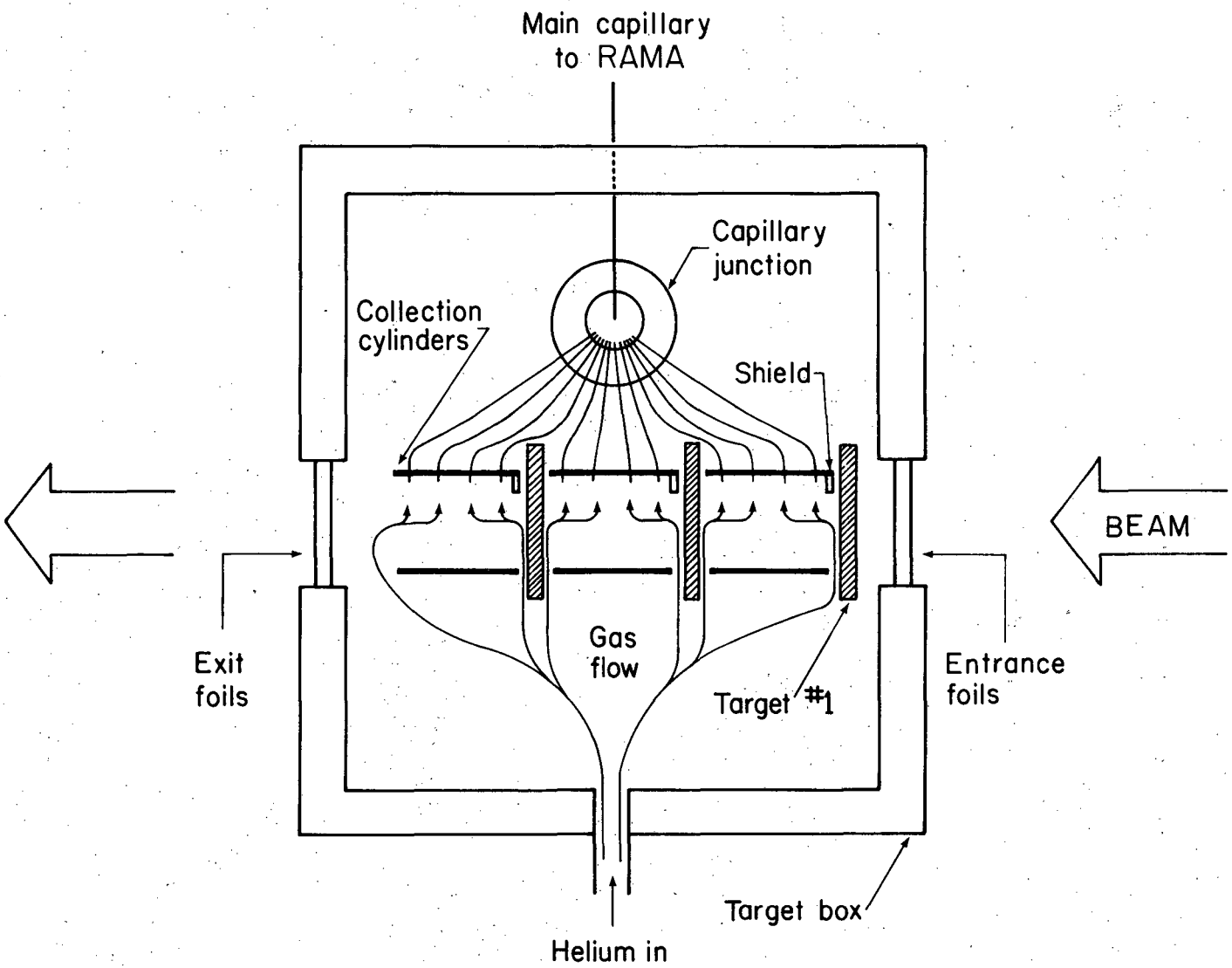

Fig. 4

XBL 793-8988

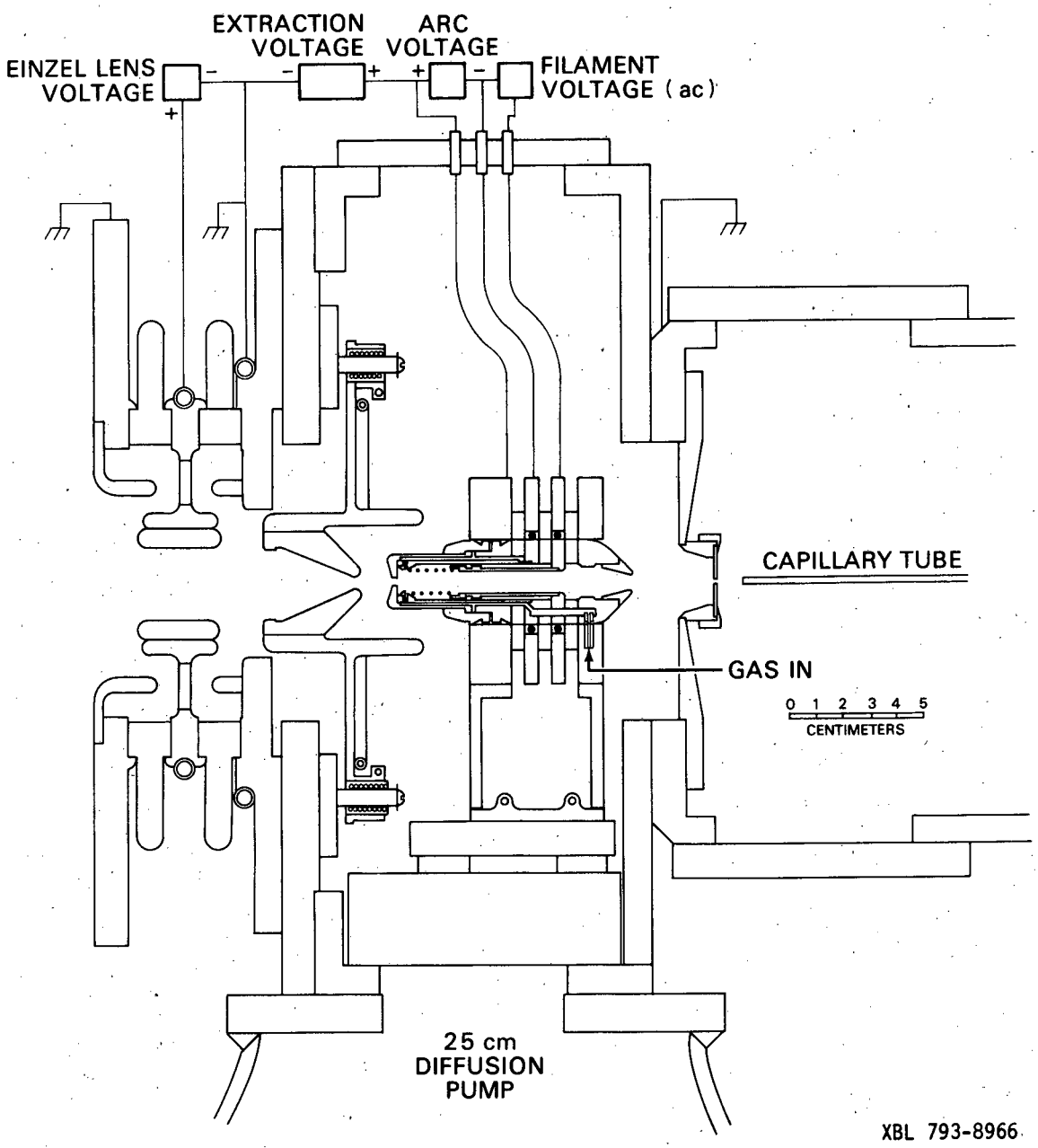

Fig. 5

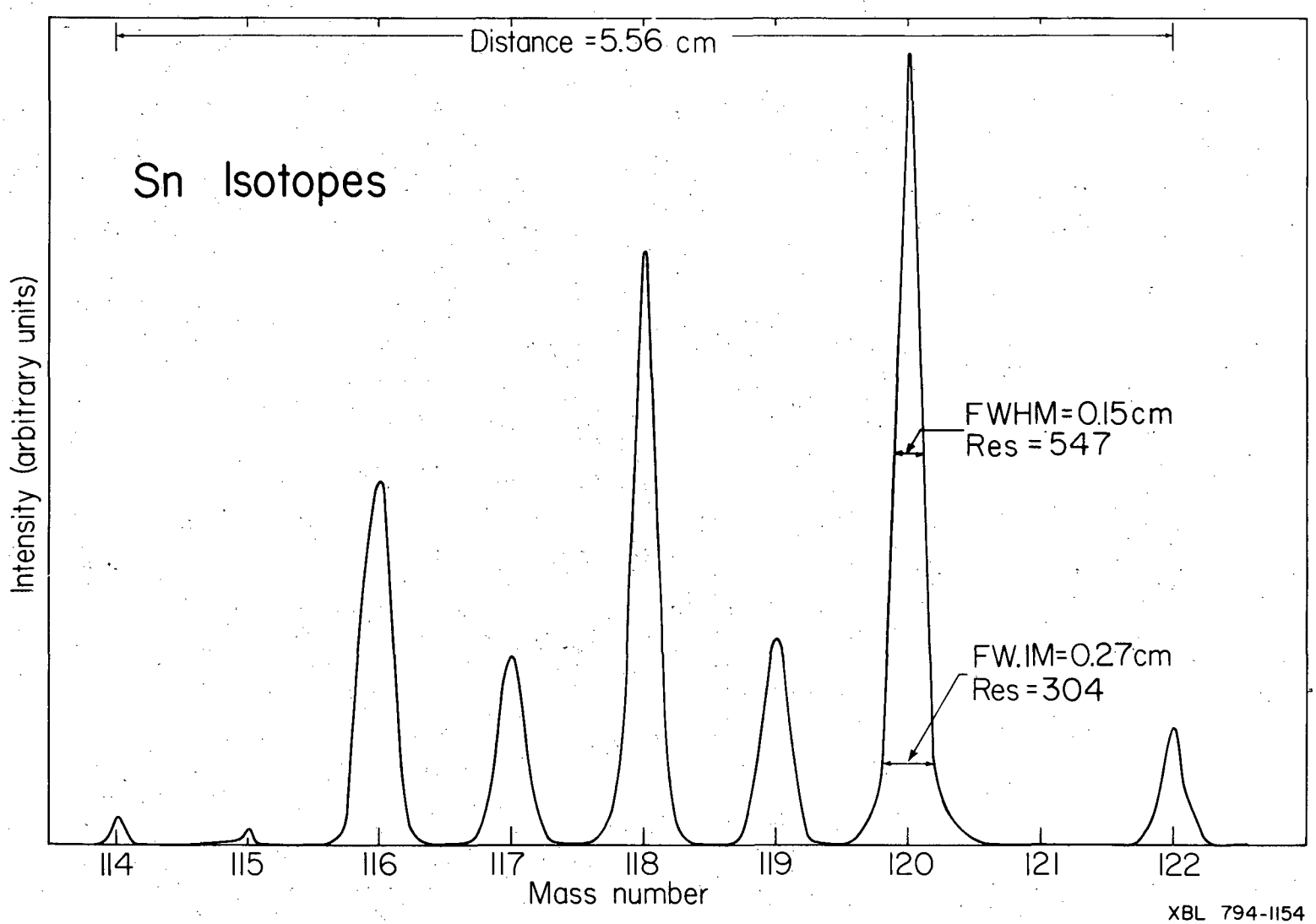
Distance =5.56 cm
Sn Isotopes
Intensity (arbitrary units)
FWHM=0.15cm
Res =547
FW.IM=0.27cm
Res =304
114
115
116
117
118
119
120
121
122
Mass number
XBL 794-1154

Fig. 6

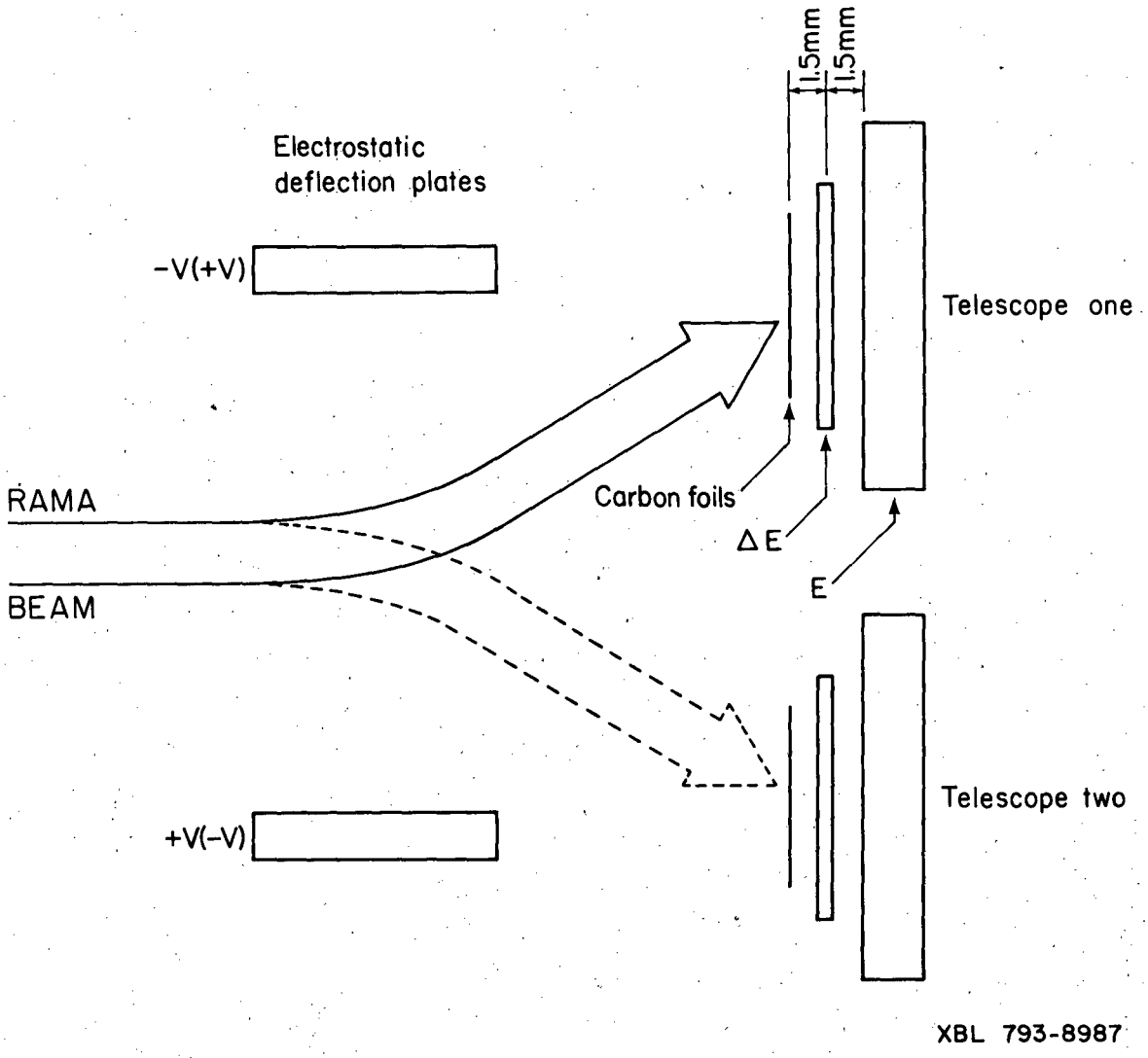

Fig. 7

U.S.GPO:1980-698-169/F-114

TECHNICAL INFORMATION DEPARTMENT
LAWRENCE BERKELEY LABORATORY
UNIVERSITY OF CALIFORNIA
BERKELEY, CALIFORNIA 94720